Supporting Information

Ultrathin black phosphorus nanosheets for efficient singlet oxygen generation

Hui Wang[1‡], Xianzhu Yang[2‡], Wei Shao[1], Shichuan Chen[1], Junfeng Xie[1], Xiaodong Zhang[1*], Jun Wang[2] and Yi Xie[1*]

[1]Hefei National Laboratory for Physical Science at the Microscale, Collaborative Innovation Center of Chemistry for Energy Materials, University of Science and Technology of China, Hefei, Anhui, 230026, P. R. China; [2]School of Life Sciences, University of Science and Technology of China, Hefei, Anhui, 230027, P. R. China.

[‡]These authors contributed equally.

Email: zhxid@ustc.edu.cn; yxie@ustc.edu.cn

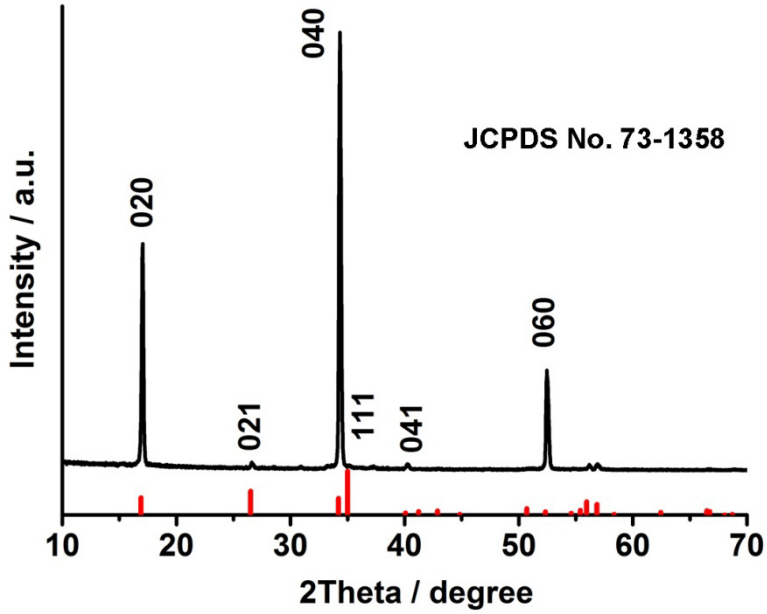

Figure S1. XRD pattern of bulk black phosphorus.

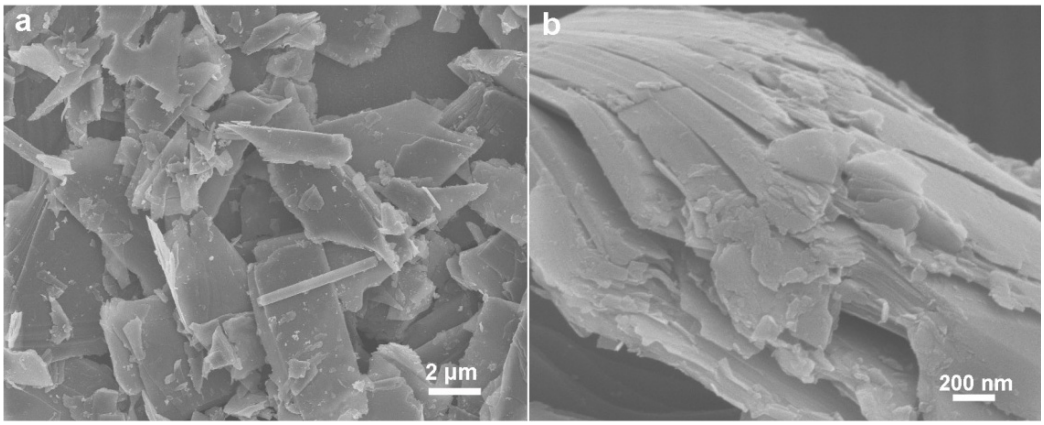

Figure S2. SEM images of the obtained bulk B.P., showing layer-stacking morphology.

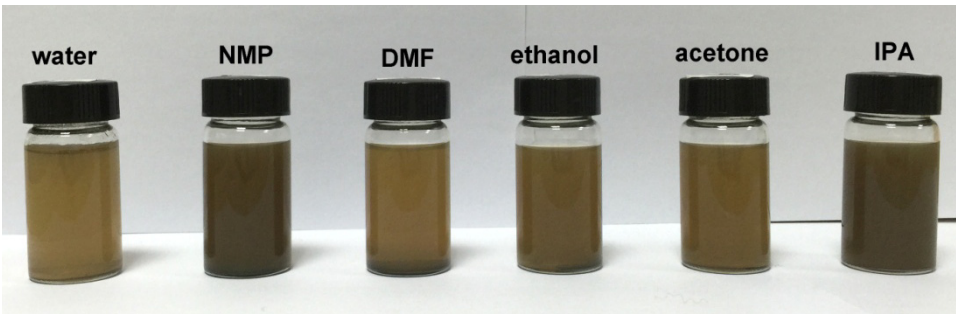

Figure S3. Photograph of as-exfoliated B.P. nanosheets dispersed in various solvents, which are water, N-methyl-2-pyrrolidone (NMP), N,N-Dimethylformamide (DMF), ethanol, acetone and isopropanol (IPA), respectively, among which the NMP is the most efficient solvent for the dispersing of B.P. nanosheets.

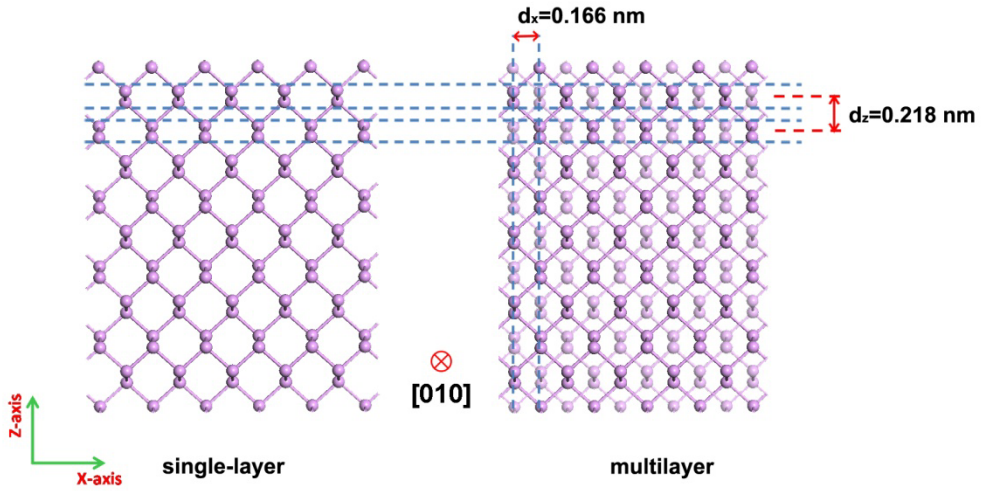

Figure S4. Atomic arrangements of single-layer and multilayer B.P. projected along [010] direction. The translucent atoms in right part mean the P-layer behind the first layer.

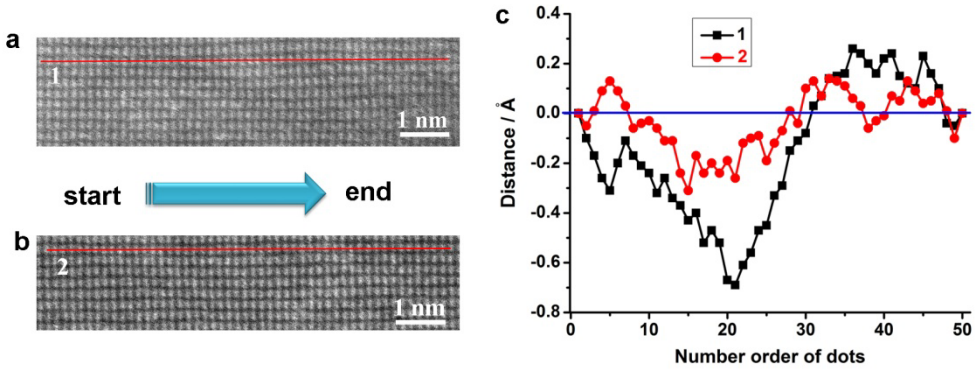

Figure S5. HAADF-STEM images analyses. (a) and (b) Radom parts of two different HAADF-STEM images. (b) Analysis the arrangement of 50 dots from (a) and (b), respectively. Herein, the zero site was defined as the middle of start and end dots. The sites of other dots that higher than the zero site were recorded as plus, otherwise, were recorded as minus.

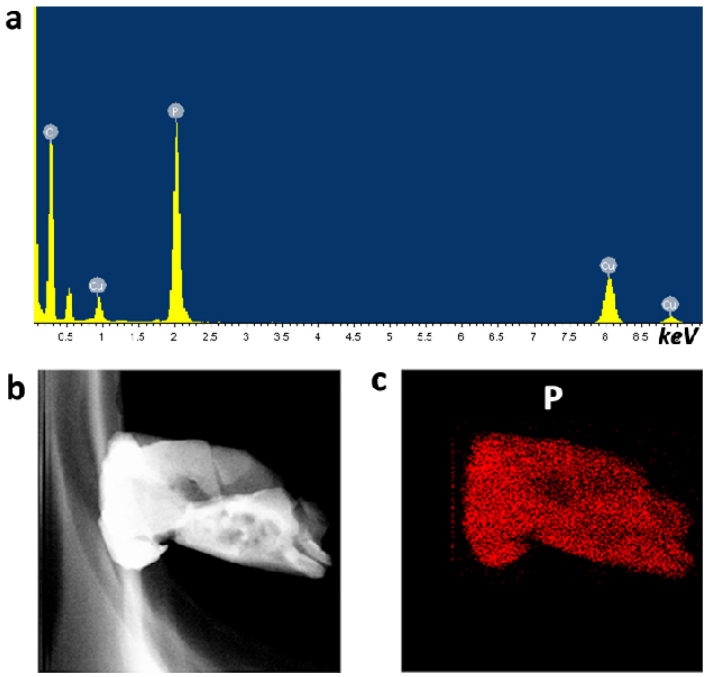

Figure S6. **Elemental analysis of exfoliated nanosheets**. (a) EDS image. (b) and (c) HAADF-STEM image and corresponding mapping image of B.P. nanosheet.

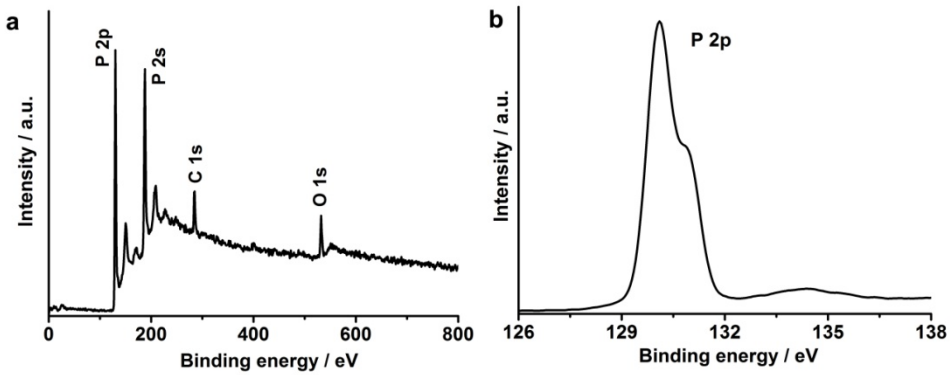

Figure S7. XPS spectra of B.P. nanosheets. (a) Survey spectrum. (b) P2p spectrum. The small peak in Fig. S7b located at about 134 eV can be assigned to P_xO_y.

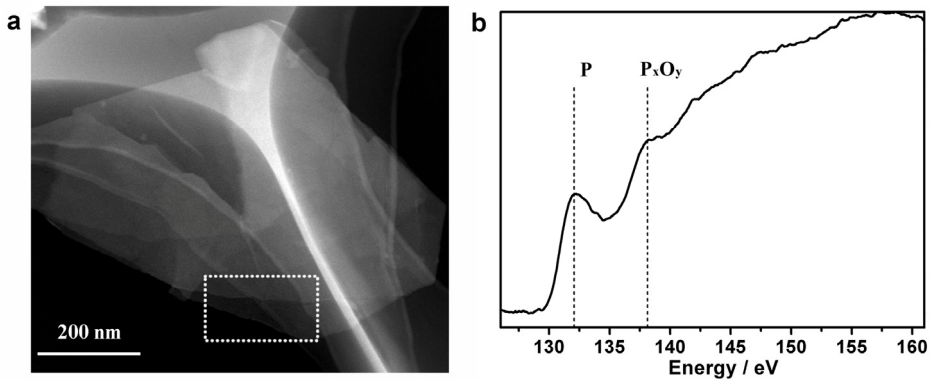

Figure S8. (a) HAADF contrast image for B.P. nanosheet, (b) corresponding EELS spectrum of the dotted box in Fig. S8a. The peak around 132 eV in EELS spectrum indicated the black phosphorus substance of obtained ultrathin nanosheet, and the peak located at 138 eV reveals the phosphorus oxides species due to the slight oxidation.

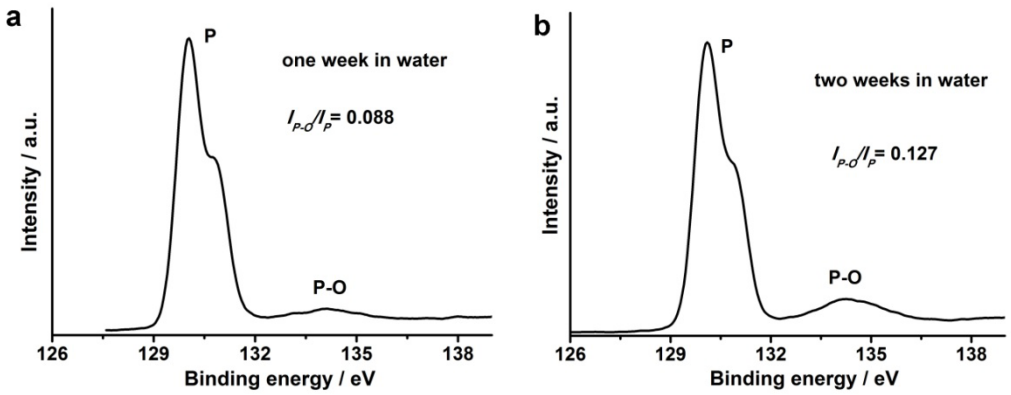

Figure S9. XPS spectra of as-exfoliated ultrathin B.P. nanosheets in water for different times. (a) one week; (b) two weeks. The peak for B.P. located at about 134 eV indicated the formation of oxidized P_xO_y.

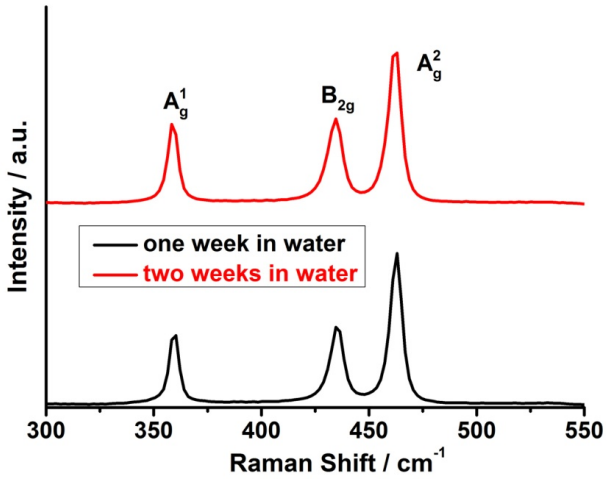

Figure S10. Raman spectra of as-exfoliated ultrathin B.P. nanosheets in water for different times.

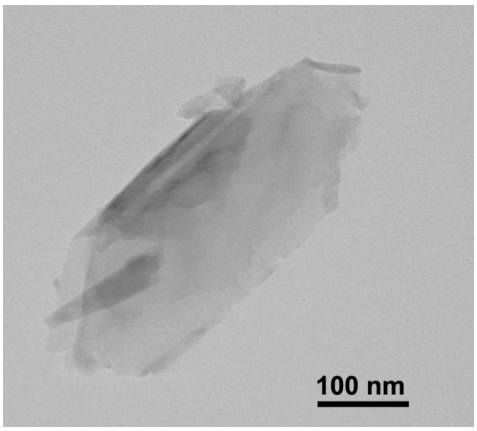

Figure S11. TEM image of ultrathin B.P. nanosheets in water for two weeks.

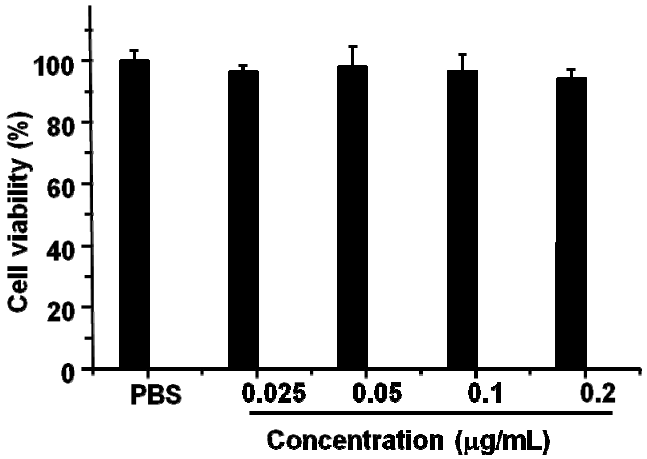

Figure S12. Viability of cells after incubation with different concentration of ultrathin B.P. nanosheets in dark.

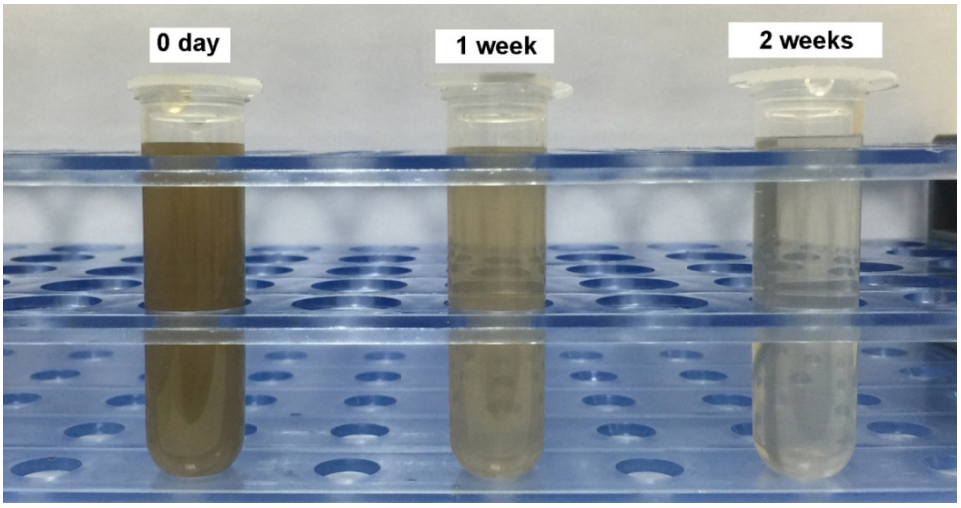

Figure S13. Photographs of the supernatant of as-exfoliated B.P. nanosheets in water for different times under light irradiation. The suspension of B.P. nanosheets was under light irradiation of about 20 minutes for every two days. From which one can see that the degradation of B.P. nanosheets in water was dramatically accelerated under light irradiation.

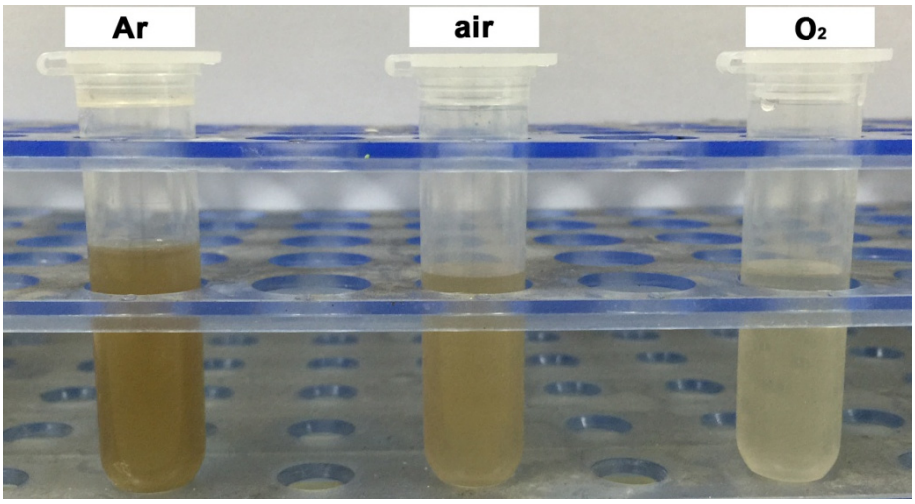

Figure S14. Photographs of the supernatant of water-exfoliated B.P. nanosheets under different atmospheres (Ar, air and O_2, respectively). The above suspension was under continuous light irradiation of about 2 hours. From which one can see that B.P. nanosheets in oxygen atmosphere show the fastest degradation rate among the three atmospheres. The results indicate that oxygen plays crucial role in the photodegradation of B.P. nanosheets.

concentration (ppm) / sample	phosphite (PO_3^{3-})	phosphate (PO_4^{3-})	other P_xO_y radial
fresh	1.84	0.42	hardly identify
1 week	10.73	1.53	
2 weeks	18.82	2.83	

Table S1. The concentrations of P_xO_y ions of the samples showed in Supplementary Fig. S13 analyzed by inductively coupled plasma emission spectroscopy (ICP) spectra. It is clear that the main product for the degradation of B.P. is phosphite in water. Beyond the identified phosphite and phosphate, there are still a few peaks in ICP spectra hardly to identify.

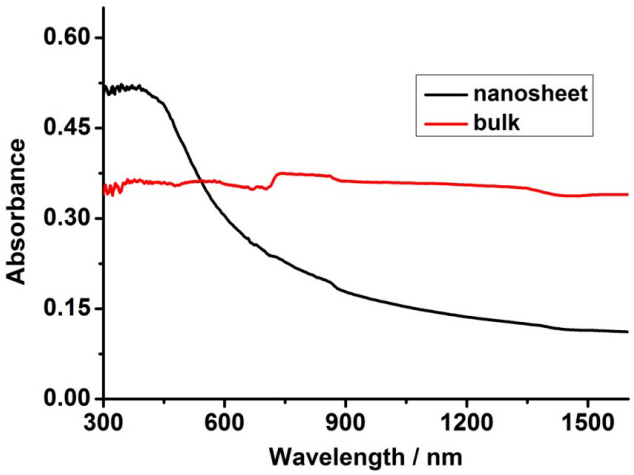

Figure S15. UV-vis spectra of bulk B.P. and ultrathin B.P. nanosheets.

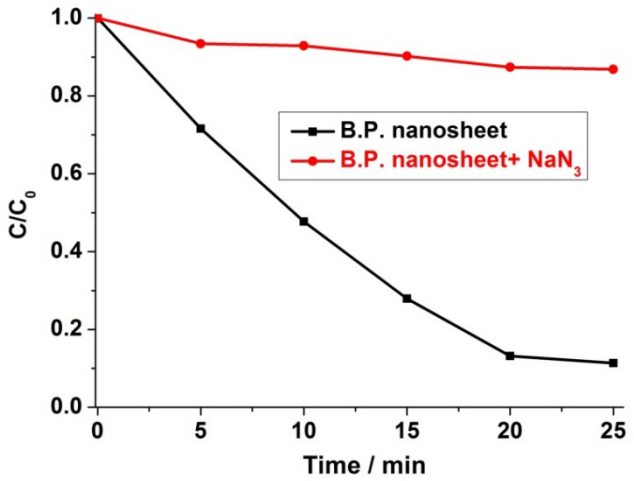

Figure S16. Photocatalytic degradation of Methyl Orange (MO) by B.P. nanosheets with or without NaN_3. Test conditions: 5 mg catalyst; 10 mg NaN_3; 100 mL MO solution with concentration of 6 mg/L, under Xe lamp with 600 nm cut-off filter.

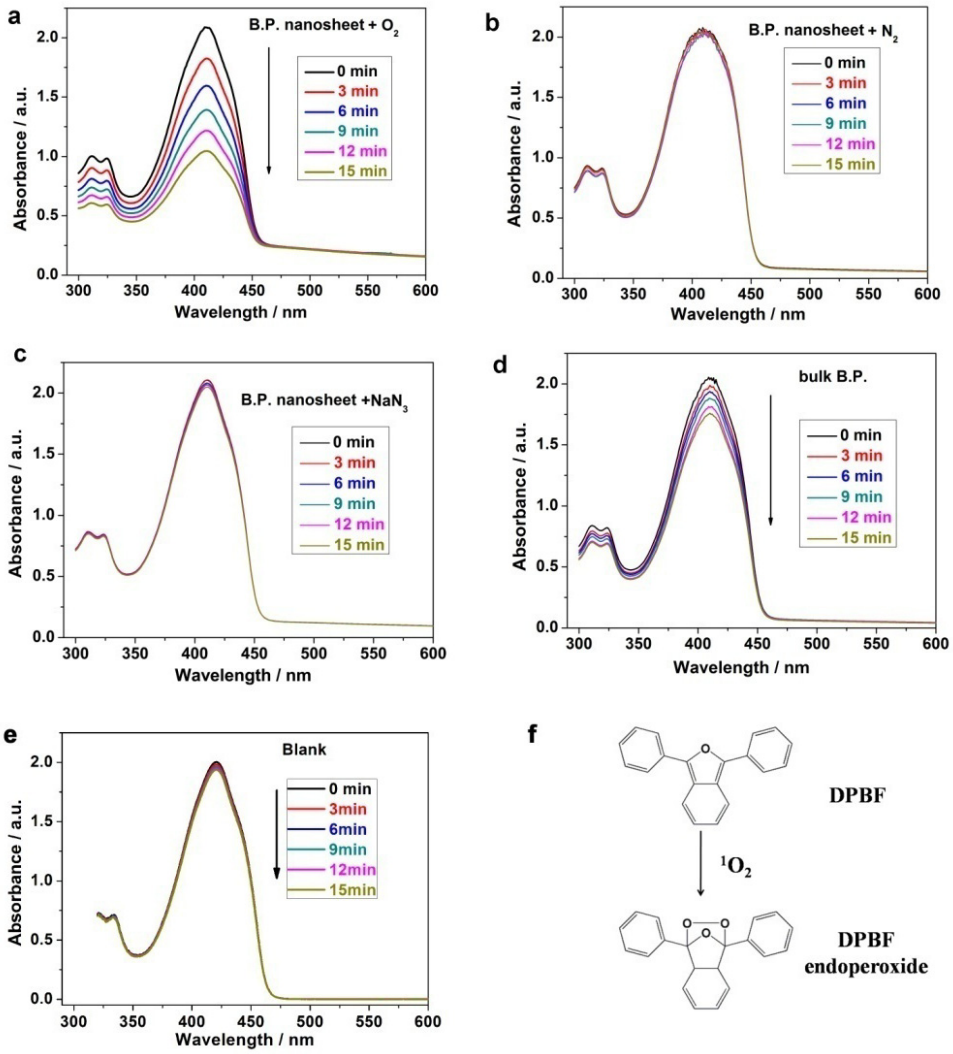

Figure S17. Time-dependent absorption spectra of the DPBF in different conditions. (a) Ultrathin B.P. nanosheets in O_2 atmosphere; (b) Ultrathin B.P. nanosheets in N_2 atmosphere; (c) Ultrathin B.P. nanosheets with adding 5 mg NaN_3; (d) Bulk B.P. in air; (e) Blank; (f) Illustration of the reaction from DPBF to DPBF endoperoxide by singlet oxygen. Test conditions: 1 mg catalyst; 100 mL DPBF solution with concentration of 20 mg/L. The reactions were conducted under Xe lamp with 600 nm cut-off filter in ethanol.

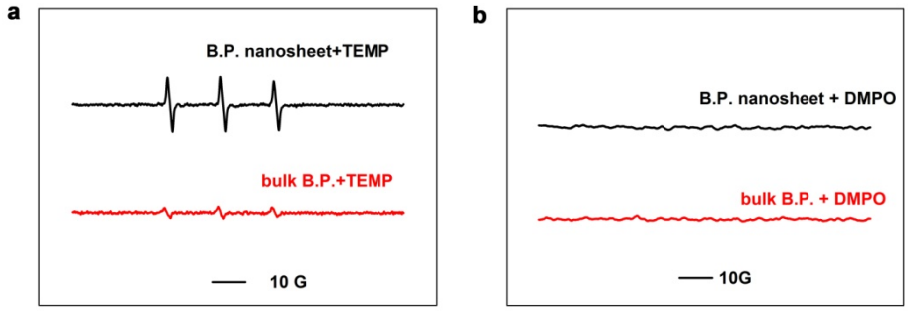

Figure S18. ESR spectra of B.P. nanosheets and bulk B.P. in the presence of (a) 2,2,6,6-tetramethylpiperidine (TEMP) and (b) 5,5-Dimethyl-1-Pyrroline-N-Oxide (DMPO) with light (Xe lamp with 600 nm cut-off filter) irradiation, respectively. The results indicate the B.P. only generate singlet oxygen under light irradiation, and no hydroxyl radicals or superoxide were generated in those system.

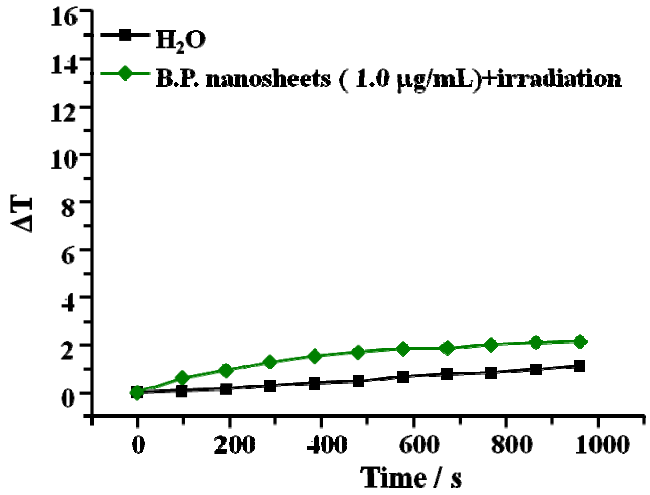

Figure S19. Photothermal effect of ultrathin B.P. nanosheets. The temperature of B.P. nanosheets suspension shows negligible photothermal effect just as pure water.

To study the photothermal effect, 500 μL solution containing ultrathin B.P. nanosheets (1.0 μg/mL) was transferred into centrifuge tube and irradiated by the 660 nm laser (BWT Beijing Ltd.) at a power density of 0.5 W cm^{-2}, while water was used as a negative control. During the NIR irradiation, the temperature of the solution was monitored by an infrared camera (ICI7320, Infrared Camera Inc.) and analyzed using IR Flash thermal imaging analysis software (Infrared Cameras Inc.).